

Virology Group, Department of Biochemistry, Monash University, (Australia). ^bINRA, Montpellier, (France). ^cSwiss Light Source at The Paul Scherrer Institute, (Switzerland). Email: fasseli.coulibaly@monash.edu

While protein crystallization of highly purified proteins has been studied for decades and used to painstakingly produce crystals for structural analysis, common insect viruses have evolved proteins that readily crystallize *in vivo* despite the complexity of the cellular environment. Viral, *in vivo* crystals are among the most striking examples of protein self-assembly, ultimately leading to the formation of ultra-stable microcrystals occupying most of the infected cells.

Recently, the first structures of *in vivo* crystals were elucidated from viral polyhedra produced by RNA [1] and DNA [2,3] viruses. The function of polyhedra is to package up to hundreds of viral particles constituting the main infectious form of the virus and allowing the virus to persist for years in the environment like bacterial spores.

Apart from polyhedra, spheroids produced by poxviruses are the only other known example of viral infectious crystals. RNA and DNA virus polyhedra share nearly identical lattices, similar function and, of course, common polyhedral morphologies. In contrast, whether spheroids were single crystals remained unclear because of their ovoid shape and the large size of their 100kDa matrix protein.

To elucidate the molecular organization of the third class of infectious crystals, we determined the 2.5Å structure of entomopoxvirus spheroids. These diffraction experiments were carried out on spheroids with maximum dimensions of 15µm directly purified from infected insects and stored frozen for over two decades.

The structure determination of spheroids confirmed that they are also single crystals despite their unusual ovoid shape. In the crystal, the main constituent of spheroids, called the spheroidin protein, adopts a multi-domain fold with five independent structural domains unrelated to either of the two types of polyhedrin protein. The asymmetric unit of the crystal contains two 100kDa spheroidin molecules adopting conformations that differ by hinge movements between the five domains. This apparent flexibility of the spheroids building blocks was totally unexpected given that crystallization occurs readily *in vivo* despite the complexity of the cellular milieu and results in remarkably stable crystals. A detailed analysis of the crystal organization provides an explanation to this conundrum revealing that building blocks interlock into the crystalline lattice using an extensive network of disulfide bonds.

In conclusion, this structure provides a detailed view of what may constitute the most improbable protein crystals. Spheroids not only harbor an atypical ovoid shape and host hundreds of irregular virus particles without disruption of the crystalline lattice but they are also able to assemble *in vivo* from large and flexible building blocks. Mirroring the complexity of poxviruses themselves, spheroids are undoubtedly the most elaborate viral armors providing a unique model of *in vivo* crystallization.

[1] F. Coulibaly et al. *Nature* **2007**, *446*, 97-101. [2] F. Coulibaly et al. *Proc Natl Acad Sci USA* **2009**, *106*, 22205-10. [3] X. Ji et al. *EMBO J* **2010**, *29*, 505-514.

Keywords: microcrystallography, virology, assembly

MS.08.5

Acta Cryst. (2011) **A67**, C37

X-ray structure of a functional full-length dynein motor domain
Genji Kurisu,^{a,b,d} Takahide Kon,^{a,b} Rieko Shimo-Kon,^a Kazuo Sutoh,^c ^aInstitute for Protein Research, Osaka University (Japan). ^bDepartment of Macromolecular Science, Graduate School of Science, Osaka University (Japan). ^cFaculty of Science and

Engineering, Waseda University (Japan). ^dPRESTO, (Japan) Science and Technology Agency (JST). E-mail: takahide.kon@protein.osaka-u.ac.jp

Dyneins are microtubule-based motor complexes that power a wide variety of biological processes within eukaryotic cells, including the beating of cilia and flagella, cell division, cell migration, and the intracellular trafficking. Compared to the other cytoskeletal motors kinesin and myosin, the molecular mechanism of dynein is still poorly understood, in part due to the lack of high-resolution structural information. Because dyneins belong to the AAA+ family of mechanochemical enzymes, its structure and mechanism must be fundamentally different from the G-protein related kinesins and myosins. The X-ray crystallography of dynein or even its motor domain—a 380-kDa portion of the heavy chain responsible for dynein's motor activity—has been challenging due to its large size and molecular complexity.

Here, we report an X-ray crystallographic analysis of the entire functional 380-kDa motor domain of *Dictyostelium* cytoplasmic dynein, the longest polypeptide (~3,300 residues) that has been crystallized so far. Diffraction from crystals extends to 4.0 Å using synchrotron radiation from an undulator source (BL44XU, SPring-8). Diffraction is consistent with space group $P2_12_12_1$ with unit cell dimensions of $a = 201.17$ Å, $b = 228.96$ Å, $c = 195.73$ Å. Based on an electron density map calculated from the Ta₆Br₁₂ derivative data at 4.5 Å resolution, an α -helical model of the dynein motor domain has been created [1]. The analysis reveals detailed architectures of functional units responsible for the motor activity, such as the ATP-hydrolyzing, ring-like head composed of six AAA+ modules as well as the long coiled-coil microtubule-binding stalk, the force-generating rod-like linker and some unpredicted structures likely to be key to function. This long sought crystal structure provides the framework to understand a large volume of data obtained by electron microscopic, biochemical and single-molecule studies, and opens the door to detailed understanding of how dynein produces force and movement.

[1] T. Kon, K. Sutoh, G. Kurisu, *Nature Struct. Mol. Biol.* **2011**, *in press*

Keywords: biomacromolecule, biophysics, mechanism

MS.09.1

Acta Cryst. (2011) **A67**, C37-C38

Generating functions for structure and chemical composition
Frank C. Hawthorne, Dept. of Geological Sciences, University of Manitoba, Winnipeg, (Canada). E-mail: frank_hawthorne@umanitoba.ca

Any crystal structure may be represented by a weighted chromatic digraph, the vertex set of which represents atoms and the edge set of which represents chemical bonds. We may write tetrahedrally coordinated cations and their associated anions as $\{T_{2n}\Theta_m\}$. For $\{T_{2n}\Theta_m\}$ to be a chain or ribbon, $5n < m \leq 6n$, and we may write m as $5n + N$, where N is an integer. Within the $\{T_{2n}\Theta_{(5n+N)}\}$ unit, we may recognize three types of anion vertices: (1) bridging anions, Θ^{br} , that are bonded to two T cations; (2) apical anions, Θ^{ap} , that are involved in linkage to other cations out of the plane of the bridging anions; and (3) linking anions, Θ^l , that link to non-T cations in the plane of the bridging anions. We can incorporate the connectivity of the cations into our algebraic representation of the chain as follows: $\{T_{2n}\Theta_a^{br}\Theta_b^{nl}\Theta_c^{ap}\}$ where $a + b + c = 5n + N$. The apical anions of the T-layer map onto a 6^3 net which, in turn, maps onto the 3^6 net of anions of the O-layer. We may use the handshaking dilemma of graph theory to examine the interaction between the two types of layers, and write a *Structure-Generating*

Function, S_n , that gives both the stoichiometry and aspects of the bond topology of the structures. We may thus write the structure-generating function, S_n , for the biopyrribole structures as follows: $S_n = X_i[M_{(3n-1)}\Psi_{2(n-1)}\{T_{2n}\Theta_{(3n-1)}^{\text{br}}\Theta_{2n}^{\text{ap}}\Theta_{2n}^{\text{br}}\}_2]$. This function generates: $n = 1$, the pyroxenes; for $n = 2$, the amphiboles; for $n = 3$, the triple-chain pyrriboles; for $n = 4$, $S_4 = X_i[M_{11}\Psi_6\{T_8\Theta_{21}\}_2]$; for $n = \infty$, the micas. Where $N = 2$, the general form of the T component is $\{T_{2n}\Theta_{5n+2}\}$ which corresponds to the T component of H-layers in the polysomatic H-O-H series in which the ribbons are linked laterally by [5]- or [6]-coordinated cations, D, which have the coordination $(D\Theta_4^{\text{ap}}\Phi_{0-1}^{\text{t}})$. The general formula for an H layer is $[D\Phi^{\text{ap}}\{T_{2n}\Theta_{3n-2}^{\text{br}}\Theta_{2n}^{\text{ap}}\Theta_{4n}^{\text{br}}\}\Phi_{0-1}^{\text{t}}]$, where Φ^{t} after the T component occurs on the outside of the H-layer and is involved in linkage between adjacent H-O-H sheets. The H-layer links via its apical anions to the O-layer, giving the general formula of an H-O-H sheet as $[M_{3n+1}D\Phi^{\text{ap}}\Psi_n\{T_{2n}\Theta_{5n+2}\}\Phi_{0-1}^{\text{t}}]$. These H-O-H sheets can link directly through the Φ^{t} anions of the $(D\Theta_4^{\text{ap}}\Phi_{0-1}^{\text{t}})$ octahedra, giving $S_n = X_i[M_{(3n+1)}\Psi_{2n}(D_2\Phi_2\{T_{2n}\Theta_{5n+2}\}_2)\Phi_{0-2}^{\text{t}}]$. This function generates: for $n = 1$, the group-1 TS-block structures; for $n = 2$, the astrophyllite-group structures; for $n = 3$, nafertisite: ideally $\text{Na}_2[\text{Fe}^{2+}_{10}\text{O}_2(\text{OH})_6(\text{Ti}_2\{\text{Si}_{12}\text{O}_{34}\})](\text{H}_2\text{O})_{0-2}$; for $n = \infty$, the micas.

We may combine the two generating functions (above) into a single function: $S_{(N+n)} = X_i[M_{(3n+2N-3)}\Psi_{2(n+N-2)}(D_{2(N-1)}\Phi_{2(N-1)}^{\text{ap}}\{T_{2n}\Theta_{(3n-N)}^{\text{br}}\Theta_{2n}^{\text{ap}}\Theta_{2N}^{\text{br}}\}_2)\Phi_{0-2(N-1)}^{\text{t}}]$ that gives all the above structures. This expression also generates mixed-ribbon polysomatic structures. $S_{(1,2+3)} = X_i[M_{13}\Psi_6\{T_{10}\Theta_{13}^{\text{br}}\Theta_{10}^{\text{ap}}\Theta_{4}^{\text{br}}\}_2]$ gives the chemical composition and structure of the mixed-chain pyrribole, chesterite: $\text{Mg}_4[\text{Mg}_{13}(\text{OH})_6\{\text{Si}_{10}\text{O}^{\text{br}}_{13}\text{O}^{\text{ap}}_{10}\text{O}^{\text{t}}_{4}\}_2]$, and $S_{(2,1+4)} = X_i[M_{17}\Psi_{10}(D_4\Phi_4\{T_2\text{O}^{\text{br}}\text{O}^{\text{ap}}\text{O}^{\text{t}}_{4}\}_2\{T_8\text{O}^{\text{br}}_{10}\text{O}^{\text{ap}}_{8}\text{O}^{\text{t}}_{4}\}_2)\Phi_{0-4}^{\text{t}}]$ gives the chemical composition and structure of the mixed-chain H-O-H mineral, veblenite: $\text{KNa}(\text{H}_2\text{O})_3[(\text{Fe}^{2+}_5\text{Fe}^{3+}_4\text{Mn}_6\text{Ca}\square)(\text{OH})_{10}(\text{Nb}_4\text{O}_4\{\text{Si}_2\text{O}_7\}_2\{\text{Si}_8\text{O}_{22}\}_2)\text{O}_2]$.

Keywords: topology, prediction, mineral

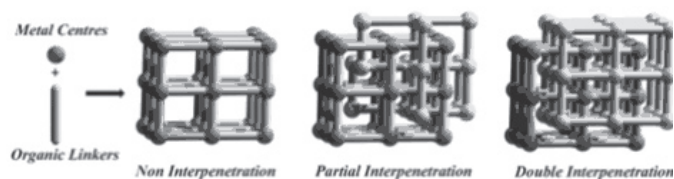
MS.09.2

Acta Cryst. (2011) A67, C38

Modulation of structures and gas storage properties in MOF materials

Martin Schröder, School of Chemistry, University of Nottingham, Nottingham NG7 2RD (UK). E-mail: M.Schroder@nottingham.ac.uk

A range of anionic metal-organic framework (MOF) materials has been prepared by combination of In(III) with tetracarboxylate isophthalate ligands. These materials incorporate organic cations, either $\text{H}_2\text{ppz}^{2+}$ (ppz = piperazine) or Me_2NH_2^+ , that are hydrogen bonded to the pore wall [1], [2]. These cations act as a gate controlling entry of N_2 and H_2 gas into and out of the porous host. Thus, hysteretic adsorption/desorption for N_2 and H_2 is observed in these systems reflecting the role of the bulky hydrogen bonded organic cations in controlling the kinetic trapping of substrates. Post-synthetic cation exchange with Li^+ leads to removal of the organic cation and the formation of the corresponding Li^+ salts. Replacement of the organic cation with smaller Li^+ leads to an increase in internal surface area and pore volume of the framework material, and in some cases to a change in the overall network topology and structure [3]. An increase in the isosteric heat of adsorption of H_2 at zero coverage has also been observed on incorporation of Li^+ ions, as predicted by theoretical modeling [4], [5], [6]. Furthermore, a new doubly-interpenetrated network system has been identified in which the second net is only partially formed (0.75 occupancy; see Figure). This material undergoes a structural re-arrangement on desolvation, and shows high selective storage uptake for CO_2 . The structures, characterisation and analyses of these charged porous materials as storage portals for gases are discussed.



- [1] S. Yang, X. Lin, A.J. Blake, K.M. Thomas, P. Hubberstey, N.R. Champness, M. Schröder *ChemComm.* **2008**, 6108- 6110. [2] S. Yang, X. Lin, A.J. Blake, G.S. Walker, P. Hubberstey, N. R. Champness, M. Schröder, *Nature Chemistry* **2009**, *1*, 487-493. [3] S. Yang, S.K. Callear, T.(A.J). Ramirez-Cuesta, W.I.F. David, J. Sun, A.J. Blake, N.R. Champness, M. Schröder, *Faraday Discussions* **2011**, in press. [4] A. Blomqvist, C.M. Araujo, P. Srepusharawoot, R. Ahuja *Proc. Natl. Acad. Sci. U.S.A.* **2007**, *104*, 20173-20176. [5] S.S. Han, W.A. Goddard *J. Am. Chem. Soc.* **2007**, *129*, 8422-8423. [6] S.S. Han, W.A. Goddard, *J. Phys. Chem. C* **2008**, *112*, 13431-13436.

Keywords: metal-organic framework, interpenetration, gas storage

MS.09.3

Acta Cryst. (2011) A67, C38-C39

New findings in topological crystal chemistry with TOPOS

Davide M. Proserpio,^a Vladislav A. Blatov,^b ^a*Università degli Studi di Milano, Dipartimento di Chimica Strutturale e Stereochimica Inorganica, Milano, (Italy)*. ^b*Inorganic Chemistry Department, Samara State University, Samara, (Russia)*. E-mail: davide.proserpio@unimi.it

The multipurpose crystallographic program TOPOS [1] has been used extensively in the analysis of entanglement of coordination polymers/MOFs and H-bonded supramolecular architectures [2], [3]. Three recent applications will be briefly illustrated.

We formalized the analysis of extended architectures by successive simplifications in an automated mode that allowed us to classify all 3-periodic structures from the Cambridge Structural Database (CSD). Different levels of representations (standard and cluster) are considered and some application illustrated. [4], [5].

Another new application of TOPOS is in the structural chemistry of intermetallic compounds, where the crystal structure is perceived as an ensemble of clusters based on convex polyhedra. We developed a computer procedure for fast automated searching for cluster fragments of any complexity in crystal structures of any nature[6]. The occurrences of two-shell clusters with the first shell as a Frank-Kasper polyhedron Z12 (dodecahedron), Z14, Z15, or Z16 (Frank-Kasper nanoclusters) will be briefly illustrated.

This latter approach has been extended in the study of zeolites, and from our result of description of all zeolites as natural tiling [7], we were able to develop a model of assembling zeolite-type frameworks as a packing of natural building units (minimal cages) or essential rings (minimal windows).

- [1] V.A. Blatov, *IUCr CompComm Newsletter* **2006**, *7*, 4-38; <http://www.topos.ssu.samara.ru>. [2] V.A. Blatov, L. Carlucci, G. Ciani, D.M. Proserpio *CrystEngComm*, **2004**, *6*, 377-395. [3] I.A. Baburin, V.A. Blatov, L. Carlucci, G. Ciani, D.M. Proserpio *Crys. Growth Des.*, **2008**, *8*, 519-539. [4] E.V. Alexandrov, V.A. Blatov, A.V. Kochetkov, D.M. Proserpio *CrystEngComm* **2011**, DOI:10.1039/C0CE00636J. [5] V.A. Blatov, D.M. Proserpio, Ch. 1 in *Modern Methods of Crystal Structure Prediction*, ed. A.R. Oganov, Wiley-VCH, Weinheim, **2011**. [6] V.A. Blatov, G.D. Ilyushin, D.M. Proserpio *Inorg. Chem.* **2010**, *49*, 1811-1818. [7] N.A. Anurova, V.A. Blatov, G.D. Ilyushin, D.M. Proserpio *J. Phys. Chem. C*, **2010**, *114*, 10160-10170.